DALTON
FULL PAPER

Synthesis, structures and dynamic NMR spectra of η^6-hexaethylbenzene complexes of ruthenium(0) and ruthenium(II)

Richard Baldwin,[a] Martin A. Bennett,*[a] David C. R. Hockless,[a] Paolo Pertici,[b] Alessandra Verrazzani,[b] Gloria Uccello Barretta,[b] Fabio Marchetti[b] and Piero Salvadori[b]

[a] *Research School of Chemistry, Australian National University, Canberra, ACT 0200, Australia*
[b] *Istituto per la Chimica dei Composti OrganoMetallici, ICCOM-CNR, Sezione di Pisa, Dipartimento di Chimica e Chimica Industriale, Università di Pisa, via Risorgimento 35, 56126 Pisa, Italy*

Received 20th May 2002, Accepted 29th August 2002
First published as an Advance Article on the web 1st November 2002

On reaction with the labile naphthalene complex [Ru(η^6-$C_{10}H_8$)(η^4-1,5-COD)], hex-3-yne undergoes stoichiometric cyclotrimerisation to form the hexaethylbenzene–ruthenium(0) complex [Ru(η^6-C_6Et_6)(η^4-1,5-COD)] **1**. In the solid state and in solution the ethyl groups adopt a 1,4-proximal-2,3,5,6-distal arrangement, as shown by X-ray crystallography and NMR (^{1}H, ^{13}C-{^{1}H}) spectroscopy. Treatment of **1** with HCl gives the binuclear ruthenium(II) complex [{RuCl(η^6-C_6Et_6)}$_2$(μ-Cl)$_2$] **2**, whose arene ligands adopt a transoid arrangement about the Ru_2Cl_2 moiety; in turn **2** reacts with methanolic NH_4PF_6 to give the salt [$Ru_2(\mu\text{-}Cl)_3(\eta^6\text{-}C_6Et_6)_2$]$PF_6$, [**3**]$PF_6$. The ethyl group conformations in crystalline **2** and [**3**]PF_6 are all-distal and 1,3,5-proximal-2,4,6-distal, respectively, whereas only the latter conformation is present in both compounds in dichloromethane or methanol solutions at low temperature according to ^{13}C-{^{1}H} NMR spectroscopy. The ν(Ru–Cl) band patterns in the IR spectra of **2** in the solid state and dichloromethane solution are almost identical, indicating that the neutral di-μ-chloro species predominates in solution at room temperature. However, the appearance at −50 °C of a resonance due to free chloride ion in the ^{35}Cl NMR spectrum of complex **2** suggests that reversible formation of [**3**]Cl may be favoured at low temperature. Dilute (*ca.* 10^{-3} M) solutions of **2** in dichloromethane and methanol behave as 1 : 1 electrolytes consistent with the presence of [**3**]Cl under these conditions. At room temperature the ethyl groups of η^6-C_6Et_6 in **1**, **2** and [**3**]PF_6 are equivalent on the NMR time-scale as a consequence of rotation about the arene–methylene bond and, possibly, rotation of the arene about the arene–metal bond. In the crystalline adducts [$RuCl_2(\eta^6\text{-}C_6Et_6)$(L)] (L = PMe_3 **4**, PPh_3 **5**) the ethyl groups are all distal and remain equivalent on the NMR time-scale in solution from room temperature to −97 °C. The results confirm conclusions, based primarily on studies of Group 6 carbonyl complexes, that the different conformations of η^6-C_6Et_6 have very similar energies.

Introduction

Hexaethylbenzene (C_6Et_6) is the smallest homosubstituted hexa-alkylbenzene that shows the effects of steric hindrance between the substituents. In the solid state the ethyl groups project alternately above and below the plane of the six-membered ring;[1,2] on η^6-coordination the ethyl groups can point either towards the metal atom (proximal) or away from it (distal). Extensive studies, especially of the Group 6 metal tricarbonyl complexes of C_6Et_6 and their derivatives, have shown the existence of a number of different conformations whose static and dynamic stereochemistry have attracted considerable interest and some controversy; a detailed review has appeared.[3] In general, the favoured conformation or conformations adopted in the solid state seem to be determined by a balance of steric effects between the ethyl groups themselves and between the ethyl groups and the ligands in the ML_n unit.

Two dynamic processes are thought to occur in η^6-C_6Et_6 metal complexes which render the distal and proximal ethyl groups equivalent in solution at room temperature: (1) uncorrelated rotation of the ethyl groups about the arene–methylene bond, and (2) rotation of the arene relative to the ML_n fragment. These processes are illustrated in Fig. 1 for [$Cr(CO)_3$(η^6-C_6Et_6)], which has a 1,3,5-proximal-2,4,6-distal arrangement of ethyl groups in the solid state;[2,4] the distal ethyl groups in this compound eclipse the Cr–CO vectors. According to

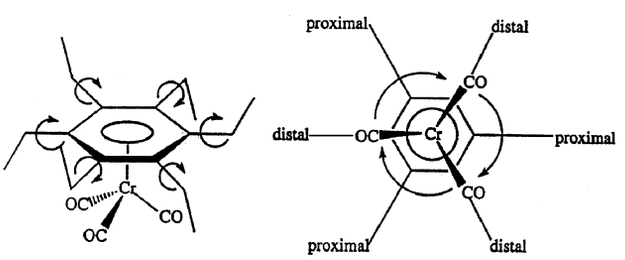

Fig. 1 Possible rotational motions in [$Cr(CO)_3(\eta^6\text{-}C_6Et_6)$].

variable temperature NMR studies of the complexes [$Cr(CO)_2$(NO)(η^6-C_6Et_6)]BF_4 and [Cr(CO)(CS)(NO)(η^6-C_6Et_6)]BF_4, the activation barriers $\Delta G^{\neq}$ to the two processes are *ca.* 39.7 and 48.1 kJ mol^{-1}, respectively.[5]

Ruthenium in both zero and +2 oxidation states forms numerous η^6-arene complexes with a variety of substituents in the aromatic ring,[6,7] but the only known η^6-C_6Et_6 complex is [Ru(η^5-C_5H_5)(η^6-C_6Et_6)]BF_4, which was isolated in poor yield from the reaction of [$Ru(CO)_2(\eta^5\text{-}C_5H_5)]_2$ with an excess of hex-3-yne in the presence of $AgBF_4$.[8,9] We describe here the synthesis and structure of some hexaethylbenzene complexes of ruthenium, with emphasis on the conformations adopted by the ethyl groups.

 DOI: 10.1039/b204875m

This journal is © The Royal Society of Chemistry 2002

Results

The usual starting compounds for entry into arene–ruthenium chemistry are the di-μ-chloro dimers, $[RuCl_2(\eta^6\text{-arene})]_2$, which, for mono- and di-substituted arenes, are generally most easily made by reaction of $RuCl_3{\cdot}xH_2O$ with the appropriate 1,3- or 1,4-cyclohexadiene. The dimeric $RuCl_2$ complexes of hexamethylbenzene,[10] tetramethylbenzene,[11,12] and 1,3,5-trialkylbenzenes are readily obtained by heating or fusing $[RuCl_2(\eta^6\text{-}p\text{-cymene})]_2$ with a large excess of the neat arene, but hexaethylbenzene does not displace *p*-cymene at 180 °C, even after 24 h, presumably because of steric hindrance. We have, therefore, adopted an alternative approach[13] based on the labile, zerovalent ruthenium complex $[Ru(\eta^6\text{-}C_{10}H_8)(\eta^4\text{-}1,5\text{-COD})]$,[14] the naphthalene ligand of which is displaced by hex-3-yne in THF at room temperature to give $[Ru(\eta^6\text{-}C_6Et_6)(\eta^4\text{-}1,5\text{-COD})]$ **1** as pale yellow crystals (eqn. (1)).

$$Ru(\eta^6\text{-}C_{10}H_8)(\eta^4\text{-}1,5\text{-}C_8H_{12}) + 3\ Et\text{-}C{\equiv}C\text{-}Et \xrightarrow[r.t.]{THF} Ru(\eta^6\text{-}C_6Et_6)(\eta^4\text{-}1,5\text{-}C_8H_{12}) + C_{10}H_8 \quad (1)$$

The complex is obtained in almost quantitative yield after chromatography and crystallisation from pentane at −78 °C and has been characterised by elemental analysis, spectroscopic measurements, and single crystal X-ray diffraction. The EI-mass spectrum shows a parent-ion peak and the ^{1}H NMR spectrum at room temperature in C_6D_6 or CD_2Cl_2 shows a quartet–triplet pattern due to apparently equivalent ethyl groups. The COD resonances appear at δ 2.76 (br s, =CH) and 2.36 (m, CH_2); in CD_2Cl_2 the former shifts to δ 2.48 and the latter appears as two 4H-multiplets centred at δ 2.04 and 1.88. These chemical shifts are similar to those of other $[Ru(\eta^6\text{-arene})(\eta^4\text{-}1,5\text{-COD})]$ complexes.[15,16] Corresponding resonances are observed in the ^{13}C-{^{1}H} NMR spectrum; the signal due to the arene carbon atoms appears at δ 103.4, *ca.* 30 ppm to low frequency of that in free C_6Et_6

It should be noted that complexes such as $[Ru(\eta^6\text{-}C_6H_6)(\eta^4\text{-}1,5\text{-COD})]$ and $[Ru(\eta^6\text{-}p\text{-cymene})(\eta^4\text{-}1,5\text{-COD})]$ do not react with hex-3-yne even in refluxing THF. The possible mechanism for this stoichiometric alkyne cyclotrimerisation has been discussed elsewhere.[13]

The molecular structure of complex **1** is shown in Fig. 2; significant bond distances and angles are listed in Table 1. The molecule has a typical piano-stool structure and the η^4-1,5-COD ligand is in its usual puckered saddle conformation. The plane containing the four olefinic carbon atoms C(19), C(20), C(23) and C(24) is almost parallel with that of the C_6Et_6 carbon atoms, the dihedral angle being 0.7(3)°. The methyl groups of the substituents at the 1- and 4- positions of the C_6Et_6 ring are proximal, those at the 2,3,5,6-positions are distal. A similar conformation has been observed in two other complexes of the type $ML_2(\eta^6\text{-}C_6Et_6)$, *viz.*, M = Ta, L = $OC_6H_3Pr^i_2$-2,6 [17] and M = Ir, $L_2 = \eta^1,\eta^3\text{-}C_8H_{13}$,[18] and in the cation of the salt $[MoCl(CO)_3(\eta^6\text{-}C_6Et_6)][MoCl_6]$.[19] In complex **1** the carbon atoms carrying the distal arms almost eclipse the olefinic carbon atoms of COD, while the proximal arms occupy the space created by the saddle-shaped conformation of COD, thus minimising steric hindrance between them and the diene. The Ru–C(COD) distances in **1** [2.133(5)–2.138(5) Å] are similar to those in $[Ru(\eta^6\text{-}C_6H_6)(\eta^4\text{-}1,5\text{-COD})]$ [2.127(4)–2.136(4) Å];[20] in contrast, the Ru–C(arene) distances are slightly greater in **1** [2.250(4)–2.265(4) Å *vs.* 2.195(7)–2.256(7) Å], presumably as a consequence of the greater bulk of C_6Et_6. In the benzene complex the aromatic ring is not completely planar but has a shallow boat conformation, as is evident from the spread of Ru–C(arene) bond lengths, whereas in **1** the Ru–C(arene) distances do not differ significantly.

Treatment of complex **1** in hexane with HCl gives the di-μ-chloro dimer $[RuCl_2(\eta^6\text{-}C_6Et_6)]_2$ **2** almost quantitatively as an orange, air-stable solid. Unlike the C_6H_6 and C_6Me_6 analogues, **2** is very soluble in dichloromethane, and fairly soluble in methanol and ethanol; solutions in CH_2Cl_2 decompose in air over a period of weeks. The peak of highest mass in the EI-mass spectrum of **2** corresponds to the loss of one chloride ion from the dimer. This process also occurs on treatment of **2** with a saturated solution of NH_4PF_6 in methanol, which gives the tri-μ-chloro salt $[Ru_2Cl_3(\eta^6\text{-}C_6Et_6)_2]PF_6$ [**3**]PF_6 as dark red crystals. The ^{1}H and ^{13}C-{^{1}H} NMR spectra of compounds **2** and [**3**]PF_6 at room temperature show the presence of equivalent ethyl groups; the arene carbon signal appears as a broad singlet at δ 94–95 (**2**) and 93–95 (**3**), *ca.* 40 ppm to low frequency of that in free C_6Et_6.

The molecular structures of complexes **2** and **3**, determined by single-crystal X-ray diffraction, are shown in Fig. 3 and 4;

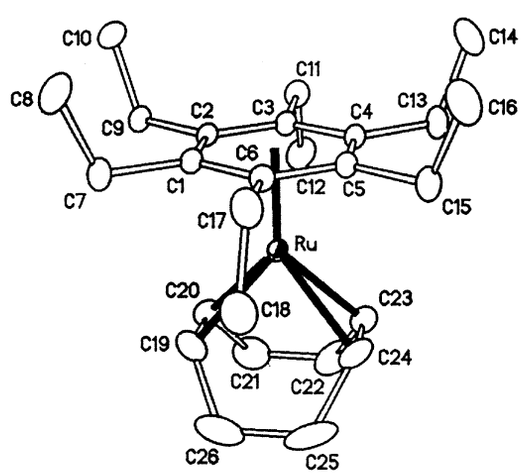

Fig. 2 An ORTEP[57] diagram of $[Ru(\eta^6\text{-}C_6Et_6)(\eta^4\text{-}1,5\text{-COD})]$ **1** showing selected atom labelling and 20% probability ellipsoids; hydrogen atoms have been omitted for clarity.

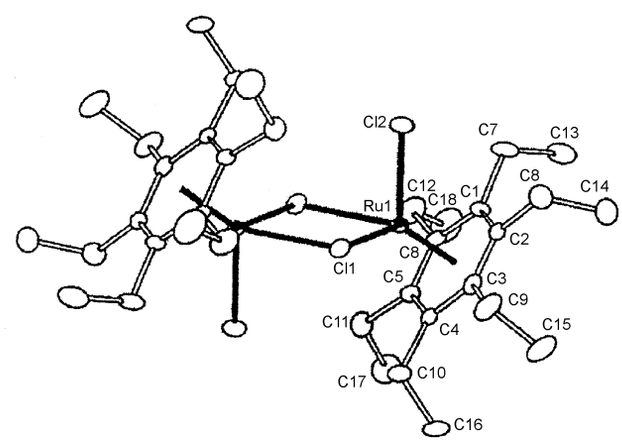

Fig. 3 An ORTEP diagram of $[RuCl_2(\eta^6\text{-}C_6Et_6)]$ **2** showing selected atom labelling and 20% probability ellipsoids; hydrogen atoms have been omitted for clarity.

selected bond lengths and angles are listed in Tables 2 and 3. Complex **2** has an edge-shared bioctahedral structure similar to those of other $[MCl_2(\eta^6\text{-arene})]_2$ complexes [M = Os, arene = *p*-cymene;[21] M = Ru, arene = C_6Me_6,[22] $C_6H_5CO_2Et$,[23] and trindane[24] (trindane = benzo(1,2:3,4:5,6)-1,2,3-trihydrocyclopentene)]. The aromatic carbon atoms of each arene ligand are coplanar, within experimental error, and these planes at the end of each molecule are parallel. The two ruthenium atoms and the two bridging chlorine atoms are coplanar; the terminal chlorine atoms are orthogonal to this plane, one above and one below it, so that the arene ligands adopt a mutually *anti* orientation. In cation **3** three bridging chlorine atoms are arranged

Table 1 Selected distances (Å) and angles (°) in [Ru(η^6-C_6Et_6)(η^4-1,5-COD)] **1**

Ru–C(19)	2.127(4)	Ru–C(20)	2.136(4)
Ru–C(23)	2.133(4)	Ru–C(24)	2.130(4)
Ru–C(1)	2.265(3)	Ru–C(2)	2.254(3)
Ru–C(3)	2.253(4)	Ru–C(4)	2.260(4)
Ru–C(5)	2.250(3)	Ru–C(6)	2.259(4)
C(19)–C(20)	1.379(7)	C(23)–C(24)	1.401(7)
C(19)–C(26)	1.490(8)	C(20)–C(21)	1.505(7)
C(21)–C(22)	1.501(9)	C(22)–C(23)	1.494(8)
C(24)–C(25)	1.518(9)	C(25)–C(26)	1.509(10)
C(1)–C(2)	1.419(5)	C(2)–C(3)	1.425(5)
C(3)–C(4)	1.431(5)	C(4)–C(5)	1.419(5)
C(5)–C(6)	1.424(5)	C(1)–C(6)	1.431(5)
Ru–C(Ar)[a]	1.750(1)	C(arom.)–CH_2	1.516(5)–1.530(5)
CH_2–CH_3	1.514(7)–1.528(5)		
C(2)–C(1)–C(6)	120.5(3)	C(1)–C(2)–C(3)	120.3(3)
C(2)–C(3)–C(4)	119.3(3)	C(5)–C(4)–C(3)	120.2(3)
C(4)–C(5)–C(6)	120.6(3)	C(5)–C(6)–C(1)	119.1(3)
C(8)–C(7)–C(1)	114.3(4)	C(2)–C(9)–C(10)	113.7(3)
C(12)–C(11)–C(3)	115.2(3)	C(4)–C(13)–C(14)	114.3(4)
C(16)–C(15)–C(5)	113.4(4)	C(18)–C(17)–C(6)	115.5(4)
C(Ar)–Ru–C(COD)[b]	79.9(2)		

[a] C(Ar) is the centroid of the aromatic ring. [b] C(COD) is the centroid of 1,5-COD.

Table 2 Selected distances (Å) and angles (°) in [$RuCl_2$(η^6-C_6Et_6)]$_2$ **2**[a]

Ru(1)–Cl(1)	2.454(2)	Ru(1)–Cl(1)′	2.460(2)
Ru(1)–Cl(2)	2.402(2)	Ru–centroid	1.638(3)
Ru(1)–C(1)	2.163(7)	Ru(1)—C(2)	2.158(7)
Ru(1)–C(3)	2.170(7)	Ru(1)–C(4)	2.193(7)
Ru(1)–C(5)	2.190(7)	Ru(1)–C(6)	2.159(7)
C(1)–C(2)	1.43(1)	C(2)–C(3)	1.405(10)
C(3)–C(4)	1.44(1)	C(4)–C(5)	1.40(1)
C(5)–C(6)	1.466(10)	C(6)–C(1)	1.42(1)
C(ar)–CH_2	1.50(1)–1.529(9)	CH_2–CH_3	1.48(1)–1.52(1)
Cl(1)–Ru(1)–Cl(1)′	80.23(7)	Cl(1)–Ru(1)–Cl(2)	86.97(7)
Cl(1)–Ru(1)–C(1)	157.0(2)	Cl(1)–Ru(1)–C(2)	118.7(2)
Cl(1)–Ru(1)–C(3)	92.7(2)	Cl(1)–Ru(1)–C(4)	92.8(2)
Cl(1)–Ru(1)–C(5)	117.4(2)	Cl(1)–Ru(1)–C(6)	156.4(2)
Cl(1)′–Ru(1)–Cl(2)	87.37(8)	Cl(1)′–Ru(1)–C(1)	122.5(2)
Cl(1)′–Ru(1)–C(2)	161.0(2)	Cl(1)′–Ru(1)–C(3)	152.2(2)
Cl(1)′–Ru(1)–C(4)	114.4(2)	Cl(1)′–Ru(1)–C(5)	90.1(2)
Cl(1)′–Ru(1)–C(6)	93.4(2)	Cl(2)–Ru(1)–C(1)	90.4(2)
Cl(2)–Ru(1)–C(2)	91.6(2)	Cl(2)–Ru(1)–C(3)	119.3(2)
Cl(2)–Ru(1)–C(4)	157.9(2)	Cl(2)–Ru(1)–C(5)	154.7(2)
Cl(2)–Ru(1)–C(6)	115.6(2)	C–C–C(arom.)	118.7(7)–121.0(6)
C(arom.)–CH_2–CH_3	112.1(7)–115.7(7)		

[a] Primed atom lies at $-x$, $-y$, $-z$.

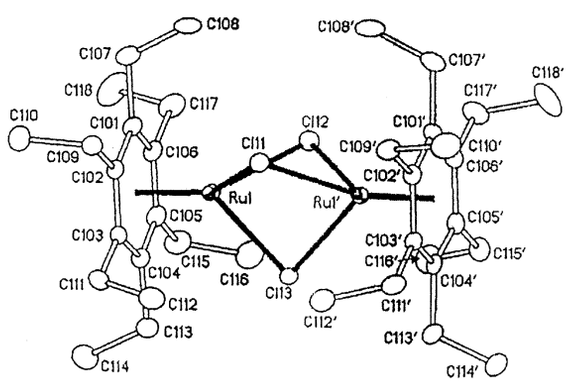

Fig. 4 An ORTEP diagram of [Ru_2Cl_3(η^2-C_6Et_6)$_2$]PF_6 [**3**]PF_6 showing selected atom labelling and 20% probability ellipsoids; hydrogen atoms have been omitted for clarity.

almost symmetrically between two ruthenium atoms in a face-sharing bioctahedral structure, the two arenes being planar and parallel to each other. Similar structures have been found for other [Ru_2Cl_3(η^6-arene)$_2$]Y salts, where arene = C_6H_6, Y = AsF_6,[25] BF_4;[26] arene = toluene, Y = BF_4;[26] arene = *p*-cymene, Y = BPh_4;[27] arene = 1,3,5-$C_6H_3Me_3$,. Y = BF_4;[28] arene = C_6Me_6, Y = PF_6.[29] When viewed along the Ru–Ru axis, three of the arene carbon atoms of cation **3** eclipse the bridging chlorine atoms; the same orientation is found in [Ru_2Cl_3(η^6-C_6H_6)$_2$]BF_4, whereas in the AsF_6 salt and in most of the other analogues mentioned above, the Ru–Cl vectors bisect the aromatic C–C bonds to give a staggered conformation. Clearly, the energy differences between different rotational isomers must be small. Whereas the ethyl groups in complex **2** adopt an all-distal arrangement, in cation **3** they are orientated in an alternating 1,3,5-proximal-2,4,6-distal conformation, with the three proximal ethyl groups occupying the space between the bridging chloride ligands, and the aromatic carbon atoms carrying the distal ethyl groups eclipsing the chloride ligands. The latter conformation is commonly observed in the solid state structures of [M(CO)$_3$(η^6-C_6Et_6)] (M = Cr, Mo)[2,4] and in derivatives in which one or two CO ligands have been replaced by analogous rod-like ligands, *e.g.* [Cr(CO)$_2$(CS)(η^6-C_6Et_6)],[30] [Cr(CO)$_2$(NO)(η^6-C_6Et_6)]BF_4,[5] [Cr(CO)(CS)(NO)(η^6-C_6Et_6)]BF_4,[5] and [{Cr(CO)$_2$(η^6-C_6Et_6)}$_2$(μ-N_2)].[31] whereas the all-distal conformation is favoured in derivatives containing fairly bulky tertiary phosphines, *e.g.* [Cr(CO)$_2$(L)(η^6-C_6Et_6)] (L = PPh_3,[2,4] PEt_3 [32]).

Table 3 Selected distances (Å) and angles (°) in $[Ru_2Cl_3(\eta^6\text{-}C_6Et_6)_2]PF_6$ [**3**]PF_6[a]

Ru(1)–Cl(11)	2.445(1)	Ru(1)–Cl(12)	2.461(1)
Ru(1)–Cl(13)	2.431(1)	Ru–centroid	1.649(2)
Ru(1)′–Cl(11)	2.447(1)	Ru(1)′–Cl(12)	2.456(1)
Ru(1)′–Cl(13)	2.430(1)	Ru(1) ··· Ru(1′)	3.3023(6)
Ru(1)–C(101)	2.190(4)	Ru(1)–C(102)	2.173(4)
Ru(1)–C(103)	2.184(5)	Ru(1)–C(104)	2.167(5)
Ru(1)–C(105)	2.189(5)	Ru(1)–C(106)	2.169(5)
Ru(1)′–C(101)′	2.191(4)	Ru(1)′–C(102)′	2.165(4)
Ru(1)′–C(103)′	2.187(4)	Ru(1)′–C(104)′	2.163(4)
Ru(1)′–C(105)′	2.187(5)	Ru(1)–C(106)′	2.168(5)
C(101)–C(102)	1.434(6)	C(102)–C(103)	1.418(6)
C(103)–C(104)	1.432(6)	C(104)–C(105)	1.420(6)
C(105)–C(106)	1.426(6)	C(106)–C(101)	1.418(6)
Cl(11)–Ru(1)–Cl(12)	79.11(4)	Cl(11)–Ru(1)–Cl(13)	79.47(4)
Cl(12)–Ru(1)–Cl(13)	79.52(4)	Ru(1)–Cl(11)–Ru(1)′	84.91(4)
Ru(1)–Cl(12)–Ru(1)′	84.38(4)	Ru(1)–Cl(13)–Ru(1)′	85.60(4)
C–C–C(arom.)[b]	117.9(4)–119.4(4)	C–C–C(arom.)[c]	120.1(4)–121.7(5)
C(arom.)–CH_2–CH_3[d]	115.8(4)–116.5(4)	C(arom.)–CH_2–CH_3[e]	108.2(4)–112.0(4)

[a] Values quoted for one independent molecule; those for second molecule do not differ significantly. [b] Carbon carrying proximal ethyl group. [c] Carbon carrying distal ethyl group. [d] Proximal ethyl group. [e] Distal ethyl group.

Variable temperature NMR spectra

Although the ethyl groups of the coordinated arene are arranged differently in complexes **1**–**3**, they are equivalent on the NMR time-scale at room temperature. We have investigated the fluxionality by variable temperature NMR spectroscopy.

On cooling a solution of complex **1** in CD_2Cl_2, the ethyl resonances broaden progressively and decoalesce between −70 °C and −80 °C (Fig. 5). At −100 °C the methyl resonance splits into two broad triplets centred at δ 1.14 and 1.36 in a 2 : 1 intensity ratio. The methylene protons at this temperature give a more complex pattern that overlaps with the =CH and CH_2 resonances of COD: there are three groups of broad signals centred at *ca.* δ 2.30, 2.04 and 1.88 together with an approximate doublet at δ 1.72, the last being due to four CH_2 protons of COD. Homonuclear decoupling experiments established that the resonance at δ 2.30 is coupled to the less intense CH_3 signal at δ 1.36 and thus contains four equivalent CH_2 (C_6Et_6) protons. The other two broad triplets, at δ 2.04 and 1.88, are coupled to each other and to the more intense methyl resonance at δ 1.14, and must, therefore, be assigned to two sets of CH_2(C_6Et_6) protons that are inequivalent in pairs (CH*H* and C*H*H).

Corresponding behaviour is observed in the variable temperature $^{13}C\text{-}\{^1H\}$ NMR spectrum of **1**. At room temperature in CD_2Cl_2 the six equivalent ethyl groups give rise to signals at δ 16.5 (CH_3), 21.2 (CH_2) and 104.0 (C_6). At −40 °C the CH_3 and C_6 signals are broad, while at −80 °C the C_6 resonance has split into two and two additional resonances appear close to the CH_2 resonance at δ 21.2. Finally, at −100 °C, there are two groups of sharp resonances, each in a 1 : 2 ratio, at δ 105.0 and 102.0 (C_6), 20.0 and 21.2 (CH_2) and 20.8 and 15.9 (CH_3), the assignments being established by a DEPT experiment.

The low temperature NMR spectra of complex **1** show that there are two ethyl group environments in a 2 : 1 ratio and are consistent with the retention in solution of the 1,4-proximal-2,3,5,6-distal conformation found in the solid state. Since each distal group is flanked by one proximal and one distal group, whereas each proximal group in flanked by a pair of distal groups, the diastereotopic methylene protons to which the protons of the four equivalent methyl groups are coupled must belong to the distal ethyl groups. The data are also consistent with the alternative 1,4-distal-2,3,5,6-proximal conformation in solution but it seems most unlikely that four methyl groups would prefer to point towards the Ru(COD) fragment. It should be noted that, if our assignment is correct, the aromatic carbon atoms bearing the distal ethyl groups are more shielded than those bearing the proximal ethyl groups and that the distal methyl carbon atoms are more shielded than the proximal ones, as found also in the $[M(CO)_3(\eta^6\text{-}C_6Et_6)]$ (M = Cr, Mo, W) complexes.[5,33] However, the proximal methylene carbon atoms in complex **1** are more shielded than the distal ones, which is the reverse of the order found in $[M(CO)_3(\eta^6\text{-}C_6Et_6)]$.

The ^1H and ^{13}C NMR spectra of complexes **2** and [**3**]PF_6 behave identically with varying temperature, in both CD_2Cl_2 and CD_3OD. The ethyl resonances at δ *ca.* 2.4 and 1.3 broaden at *ca.* −5 °C, collapse into the baseline, and re-appear at −30 °C; at −59 °C there are two triplets of equal intensity for the methyl protons and two quartets of equal intensity for the methylene protons. The average positions of each of the two new resonances coincide approximately with the respective chemical shifts at room temperature. Correspondingly, in the $^{13}C\text{-}\{^1H\}$ NMR spectra, the single methyl, methylene, and aromatic carbon resonances broaden, collapse, and re-appear at −30 °C; at −59 °C there are two triplets of equal intensity for the methyl protons and two quartets of equal intensity for the methylene protons. The average positions of each of the two new resonances coincide approximately with the respective chemical shifts at room temperature. For complex [**3**]PF_6 these observations are consistent with retention in solution of the 1,3,5-proximal-2,4,6-distal conformation of ethyl groups found in the solid state, in which the bridging Ru–Cl bonds eclipse the distal ethyl groups. In contrast, the variable temperature NMR spectra of **2** are evidently not consistent with the all-distal ethyl group conformation found in the solid state. If the molecule had retained its solid state structure in solution at low temperature, and if rotation about arene–methylene or arene–ruthenium bonds had slowed on the NMR time-scale, there should have been three different ethyl group environments in a 1 : 1 : 1 ratio.

Nature of $[RuCl_2(\eta^6\text{-}C_6Et_6)]_2$ in solution

One possible explanation of the NMR result is that, in solution, complex **2** exists predominantly as the chloride salt of cation **3**, *i.e.* $[Ru_2(\mu\text{-}Cl)_3(\eta^6\text{-}C_6Et_6)_2]Cl$, the cation being assumed to have the same 1,3,5-proximal-2,4,6-distal conformation of ethyl groups found in the PF_6 salt. We initially examined this possibility by carrying out conductivity measurements. Stephenson *et al.*[34,35] have reported that the molar conductivities (Λ_M) of 10^{-3} M solutions of $[Ru_2Cl_3(\eta^6\text{-}C_6H_6)_2]PF_6$ and $[Ru_2Cl_3(\eta^6\text{-}1,3,5\text{-}C_6H_3Me_3)_2]BF_4$ in nitromethane are, respectively, 82 and 77 S cm^2 mol^{-1}, typical of 1 : 1 electrolytes in this solvent. Measurements of Λ_M for complexes **2** and [**3**]PF_6 were made over a range of concentrations (up to 2.6×10^{-3} M for **2** and 2.5×10^{-2}M for [**3**]PF_6) in methanol. Plots of Λ_M *vs.* $c^{1/2}$ were linear, the derived

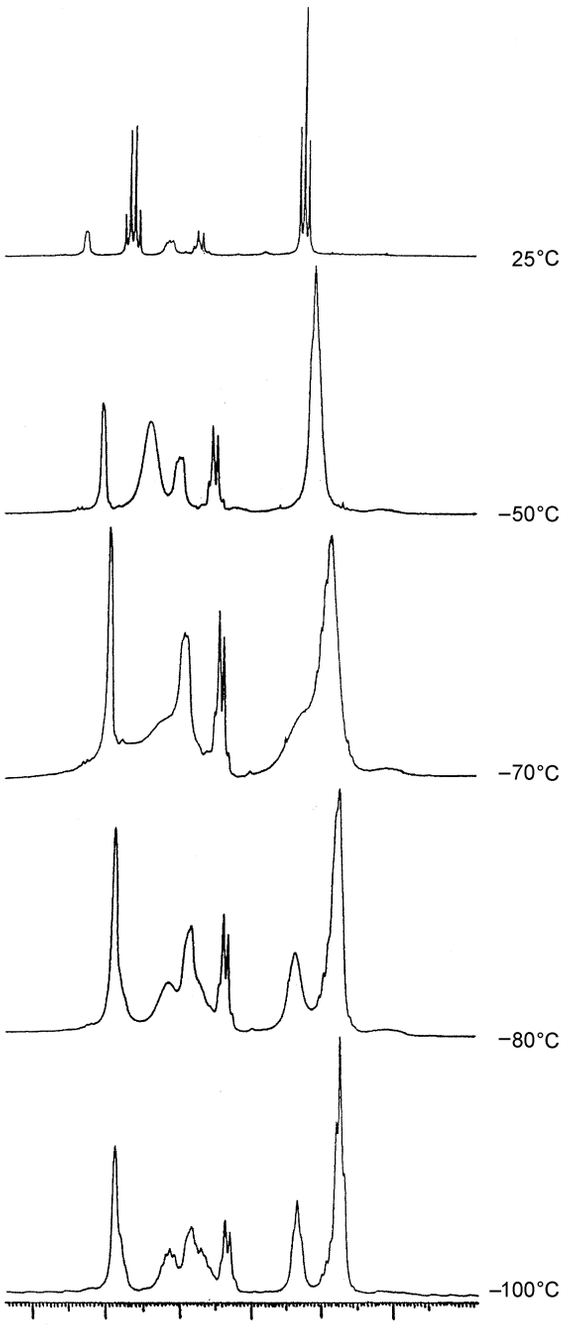

Fig. 5 Variable temperature ^{1}H NMR spectrum of [Ru(η^6-C_6Et_6)(η^4-1,5-COD)] **1**.

values of Λ_M (10^{-3}M) and Λ_0 (the molar conductivity at infinite dilution) being 75 and 117 S cm^2 mol^{-1}, respectively, for **2**, 103 and 112 S cm^2 mol^{-1} respectively, for [**3**]PF_6; these values are in the expected range for 1 : 1 electrolytes in methanol.[36] The linearity of the plots confirms that the complexes do not undergo multiple dissociations.[37] In the case of [**3**]PF_6, the slope of the $\Lambda_0 - \Lambda_M$ *vs.* $c^{1/2}$ plot is 266, which compares well with reported values for 1 : 1 electrolytes in methanol, *e.g.*, 288 for $[Ru_2Cl_3(PEt_2Ph)_6]Cl$;[37] however, for **2** the slope is greater, 1245, presumably reflecting greater ion-pairing or covalent binding of Cl compared with PF_6. Ion pairing is likely to be even more significant in dichloromethane in which solvent Λ_M values were measured over a range up to 4×10^{-3} M for **2** and 1×10^{-3} M for [**3**]PF_6; plots of Λ_M *vs.* $c^{1/2}$ were again linear. The derived values of Λ_0 were 68 and 100 S cm^2 mol^{-1}, respectively, to be compared with 120 S cm^2 mol^{-1} for $[Et_4N]Cl$ measured under similar conditions. The values of Λ_M (10^{-3} M) for **2** and [**3**]PF_6 were *ca.* 50 S cm^2 mol^{-1}, about double the values reported previously for chloride salts of complex rhodium(I) cations in CH_2Cl_2.[38] Thus, solutions of complex **2** (*ca.* 10^{-3}M) in CH_2Cl_2 or methanol appear to contain the ions $[Ru_2Cl_3(\eta^6\text{-}C_6Et_6)_2]^+$ and Cl^- in equilibrium with undissociated **2**, although whether the latter is present as an ion-pair or the neutral chloro-bridged dimer is not determined by the experiments.

Two additional pieces of evidence suggest that dissociation of chloride ion from complex **2** may also occur at higher concentrations. First, the molecular weight of a 1.9×10^{-2} M solution of **2** in CH_2Cl_2 measured by vapour pressure osmometry at 37 °C was 670 (calc. 836). Second, although the ^{35}Cl NMR spectrum of **2** in CD_3OD is very broad at room temperature, as expected for a compound containing covalently bound chloride (^{35}Cl: $I = 3/2$; $Q = -8.2 \times 10^{-30}$ m^2),[39,40] at −50 °C a new, much sharper signal appears that can be assigned to unbound chloride ion. Complex [**3**]PF_6 does not show this resonance under the same conditions. In CD_2Cl_2 the new signal is again evident at −50 °C, though observation is hampered by the large excess of covalently bound chloride in the solvent. At −75 °C the line-width is *ca.* 200 Hz, which is much less than expected for covalently bound chloride. The same sharp resonance is observed at room temperature in a solution of $[Et_4N]Cl$ in CH_2Cl_2, but it does not appear in CH_2Cl_2 alone.

There are two possible interpretations of these observations: (a) dissociation of chloride ion from complex **2** is rapid on the NMR time-scale at room temperature and slow below −50 °C, and (b) dissociation is slow on the NMR time-scale even at room temperature but the equilibrium shifts in favour of $[Ru_2Cl_3(\eta^6\text{-}C_6Et_6)_2]^+Cl^-$ as the temperature is lowered, so that only at −50 °C can the resonance due to free chloride ion be detected. The second interpretation is supported by the observation that solutions of $[RuCl_2(\eta^6\text{-trindane})]_2$ in CD_2Cl_2 contain two species in equilibrium that McGlinchey *et al.*[24] assigned to $[RuCl_2(\eta^6\text{-trindane})]_2$ and $[Ru_2Cl_3(\eta^6\text{-trindane})_2]Cl$ on the basis that the second species is favoured at lower temperatures and in the more polar solvent CD_3NO_2. If this interpretation is correct, reversible loss of chloride ion must be slow on the NMR time-scale.

The most clear-cut information about the nature of $[RuCl_2(\eta^6\text{-}C_6Et_6)]_2$ in dichloromethane solution comes from IR spectroscopy. The IR spectrum of complex **2** in the region 500–150 cm^{-1} is essentially identical in the solid state and in CH_2Cl_2, and contains three strong absorptions at 365, 310 and 240 cm^{-1} due to ν(Ru–Cl) vibrations. In the same region, complex [**3**]PF_6 shows just two strong bands at 310 and 240 cm^{-1}, which must be due to bridging Ru–Cl modes [$\nu(Ru\text{–}Cl_{br})$]; hence, the band at 365 cm^{-1} in the spectrum of **2** is due to a terminal Ru–Cl mode [$\nu(Ru\text{–}Cl_t)$]. Similarly, the spectrum of $[RuCl_2(\eta^6\text{-}C_6Me_6)]_2$, both as a solid and in CH_2Cl_2, shows three strong bands at *ca.* 340 cm^{-1} [$\nu(Ru\text{–}Cl_t)$], 300 cm^{-1} [$\nu(Ru\text{–}Cl_{br})$] and 240 cm^{-1} [$\nu(Ru\text{–}Cl_{br})$], whereas $[Ru_2Cl_3(\eta^6\text{-}C_6Me_6)_2]PF_6$ shows only two strong bands at *ca.* 280 cm^{-1} and 230 cm^{-1} [Pandey *et al.*[29] report a band due to ν(Ru–Cl) at 265 cm^{-1}, similar to the values obtained for other $[Ru_2Cl_3(\eta^6\text{-arene})_2]^+$ salts[41]]. Surprisingly, the $\nu(Ru\text{–}Cl_t)$ frequencies for $[RuCl_2(\eta^6\text{-}C_6Me_6)]_2$, and especially $[RuCl_2(\eta^6\text{-}C_6Et_6)]_2$, are considerably higher than those reported for $[RuCl_2(\eta^6\text{-arene})]_2$ complexes containing less highly substituted arenes (*ca.* 300 cm^{-1}),[41] but the assignment seems secure and there is no obvious explanation.

In summary, the main species present in dichloromethane solutions of $[RuCl_2(\eta^6\text{-}C_6Et_6)]_2$ is the chloro-bridged dimer, although $[Ru_2Cl_3(\eta^6\text{-}C_6Et_6)_2]Cl$ may become a significant component in very dilute solutions and at low temperature. In solution, the ethyl groups in the dimer adopt the 1,3,5-distal-2,4,6-proximal conformation, in contrast to the all-distal conformation found in the solid state.

Tertiary phosphine derivatives of $[RuCl_2(\eta^6\text{-}C_6Et_6)]_2$ 2

Replacement of one of the carbonyl ligands of $[Cr(CO)_3(\eta^6\text{-}C_6Et_6)]$ by tertiary phosphines of increasing bulk causes a systematic change in the original 1,3,5-distal-2,4,6-proximal conformation of ethyl groups. Thus, the solid-state conformations in $[Cr(CO)_2(L)(\eta^6\text{-}C_6Et_6)]$ are 1,2,3,5-distal-2,4-proximal (L = PMe_3),[42] 1,2,3,4,5-distal-6-proximal and all-distal (equal populations) (L = PEt_3),[32] and all-distal (L = PPh_3).[2,4] In the PMe_3 derivative, four stereoisomers can be detected by $^{31}P\text{-}\{^1H\}$ NMR spectroscopy at low temperature, that found in the solid state being the least populated in solution. It was of interest to see whether the Ru–C_6Et_6 system would show similar behaviour.

Complex **2** reacts with a stoichiometric amount of PMe_3 in refluxing toluene, or with a slight excess of PPh_3 in refluxing dichloromethane, to give the adducts $[RuCl_2(L)(\eta^6\text{-}C_6Et_6)]$ (L = PMe_3 **4**, PPh_3 **5**) as orange-red, air-stable, crystalline solids. They show singlets in their $^{31}P\text{-}\{^1H\}$ NMR spectra in CD_2Cl_2 at δ 3.1 and 24.0, respectively, which are fairly close to the values reported for the corresponding C_6Me_6 complexes (δ 0.6 in $CDCl_3$ for L = PMe_3,[43] δ 29.3 in $CDCl_3$, 30.4 in CD_2Cl_2 for L = PEt_3 [44]), and the spectrum of **4** remained unchanged down to −60 °C. The ^1H and $^{13}C\text{-}\{^1H\}$ NMR spectra show the presence of equivalent ethyl groups and the signal due to the coordinated arene carbon atoms appears at δ *ca.* 100 without discernible ^{31}P coupling. Unlike the spectra of complexes **1**–**3**, those of **4** and **5** are invariant with temperature.

The X-ray structures of complexes **4** and **5** are shown in Fig. 6 and 7; selected bond distance and angles are listed in Tables 4

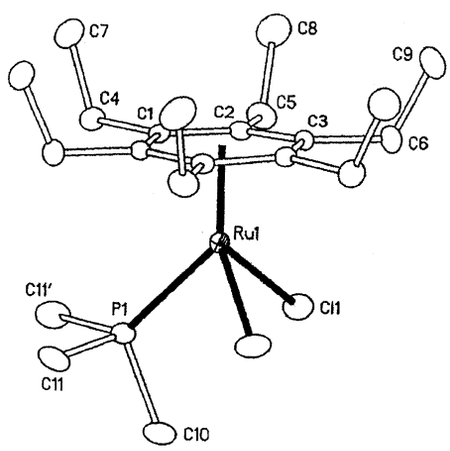

Fig. 6 An ORTEP diagram of $[RuCl_2(PMe_3)(\eta^6\text{-}C_6Et_6)]$ **4** showing selected atom labelling and 20% probability ellipsoids; hydrogen atoms have been omitted for clarity.

and 5. Both complexes have the expected half-sandwich, piano-stool structure with the arene ethyl groups in the all-distal conformation. When viewed along the arene–Ru bond axis, the ligand tripod is staggered relative to the arene carbon atoms. The Ru–arene(centroid) distance is significantly greater in **5** [1.720(2) Å] than in **4** [1.696(1) Å], possibly reflecting greater steric hindrance to arene coordination induced by the larger tertiary phosphine. In agreement, the Ru–P distance in **5** [2.388(1) Å] is greater than that in **4** [2.343(1) Å], *cf.* 2.3637(12) Å in $[RuCl_2(PPh_3)(\eta^6\text{-}C_6H_6)]$.[45] The Ru–C(arene) distances span the ranges 2.196(3)–2.251(3) Å for **4** and 2.207(5)–2.252(5) Å for **5** but, in contrast to the η^6-benzene complexes $[RuCl_2(L)(\eta^6\text{-}C_6H_6)]$ (L = $PMePh_2$,[46] PPh_3 [45]), there is no systematic lengthening to the carbon atoms *trans* to the tertiary phosphine.

Discussion

The compound $[Ru(\eta^6\text{-}C_6Et_6)(\eta^4\text{-}1,5\text{-}COD)]$ **1** is readily prepared by the stoichiometric cyclotrimerisation of hex-3-yne on

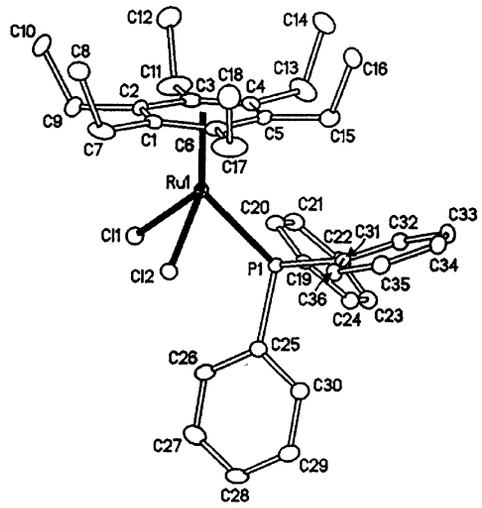

Fig. 7 An ORTEP diagram of $[RuCl_2(PPh_3)(\eta^6\text{-}C_6Et_6)]$ **5** showing selected atom labelling and 20% probability ellipsoids; hydrogen atoms have been omitted for clarity.

Table 4 Selected distances (Å) and angles (°) in $[RuCl_2(PMe_3)(\eta^6\text{-}C_6Et_6)]$ **4**

Ru(1)–Cl(1)	2.4181(9)	Ru(1)–P(1)	2.343(1)
Ru(1)–C(1)	2.200(3)	Ru(1)–C(2)	2.196(3)
Ru(1)–C(3)	2.251(3)	C(1)–C(1a)	1.431(6)
C(1)–C(2)	1.416(4)	C(2)–C(3)	1.440(4)
C(3)–C(3a)	1.416(6)		
Cl(1)–Ru(1)–Cl(1a)	90.35(5)	Cl(1)–Ru(1)–P(1)	82.11(3)
Cl(1)–Ru(1)–C(1)	115.83(8)	Cl(1)–Ru(1)–C(2)	88.96(8)
Cl(1)–Ru(1)–C(3)	89.81(7)	Cl(1)–Ru(1)–C(1a)	153.79(8)
Cl(1)–Ru(1)–C(2a)	154.03(8)	Cl(1)–Ru(1)–C(3a)	116.28(8)
P(1)–Ru(1)–C(1)	99.51(8)	P(1)–Ru(1)–C(2)	123.43(8)
P(1)–Ru(1)–C(3)	160.08(8)		

Table 5 Selected distances (Å) and angles in $[RuCl_2(PPh_3)(\eta^6\text{-}C_6Et_6)]$ **5**

Ru(1)–Cl(1)	2.423(1)	Ru(1)–Cl(2)	2.412(1)
Ru(1)–P(1)	2.388(1)	Ru(1)–C(1)	2.235(5)
Ru(1)–C(2)	2.242(5)	Ru(1)–C(3)	2.207(5)
Ru(1)–C(4)	2.234(5)	Ru(1)–C(5)	2.252(5)
Ru(1)–C(6)	2.217(5)	C(1)–C(2)	1.403(7)
C(2)–C(3)	1.454(8)	C(3)–C(4)	1.395(7)
C(4)–C(5)	1.423(7)	C(5)–C(6)	1.414(7)
Cl(1)–Ru(1)–Cl(2)	87.99(4)	Cl(1)–Ru(1)–P(1)	86.83(5)
Cl(1)–Ru(1)–C(1)	113.3(2)	Cl(1)–Ru(1)–C(2)	87.6(1)
Cl(1)–Ru(1)–C(3)	89.3(1)	Cl(1)–Ru(1)–C(4)	117.6(2)
Cl(1)–Ru(1)–C(5)	154.4(1)	Cl(1)–Ru(1)–C(6)	150.9(2)
Cl(2)–Ru(1)–P(1)	82.63(4)	Cl(2)–Ru(1)–C(1)	89.3(1)
Cl(2)–Ru(1)–C(2)	114.9(1)	Cl(2)–Ru(1)–C(3)	153.0(2)
Cl(2)–Ru(1)–C(4)	154.3(2)	Cl(2)–Ru(1)–C(5)	117.4(1)
Cl(2)–Ru(1)–C(6)	89.7(1)	P(1)–Ru(1)–C(1)	158.1(2)
P(1)–Ru(1)–C(2)	161.4(2)	P(1)–Ru(1)–C(3)	124.0(2)
P(1)–Ru(1)–C(4)	100.3(1)	P(1)–Ru(1)–C(5)	99.2(1)
P(1)–Ru(1)–C(6)	121.6(1)		

ruthenium(0) and is easily converted into $[RuCl_2(\eta^6\text{-}C_6Et_6)]_2$ **2**. The availability of this precursor should enable the conformational and dynamic properties of hexaethylbenzene in its ruthenium and Group 6 transition metal complexes to be compared. The 1,4-proximal-2,3,5,6-distal arrangement of ethyl groups found in complex **1** has not been observed so far in any complexes of the $[M(CO)_3(\eta^6\text{-}C_6Et_6)]$ class, thus illustrating how the conformation is determined primarily by the auxiliary ligand array (bipodal in the case of **1**). While complexes **1** and **[3]**PF_6 appear to retain in solution the ethyl group conformations found in the solid state (1,3,5-proximal-2,4,6-distal for the latter), the evidence suggests that in complex **2** the conformation changes from all-distal in the solid to 1,3,5-proximal-

2,4,6-distal in solution at low temperature. The energies of the various conformations are clearly similar and several examples of similar changes are known. For example, the cation $[Fe(\eta^5\text{-}C_5H_5)(\eta^6\text{-}C_6Et_6)]^+$ adopts a 1,3-proximal-2,4,5,6-distal ethyl group conformation in its PF_6 salt [47] and a 1-proximal-2,3,4,5,6-distal conformation in its BPh_4 salt,[48] while in solution at low temperature these co-exist with a third isomer having an all-distal conformation.[49] In contrast, $[Ru(\eta^5\text{-}C_5H_5)(\eta^6\text{-}C_6Et_6)]PF_6$ appears to adopt the 1,3,5-proximal-2,4,6-distal conformation in solution, though the conformation in the solid state in unknown.[8,9] It seems likely that conformations, such as 1,3-proximal-2,4,5,6-distal, 1-proximal-2,3,4,5,6-distal, and all-distal are present in equilibrium with 1,3,5-proximal-2,4,6-distal in solutions of complexes **2** and **[3]**PF_6 above *ca.* −50 °C; interconversion at an intermediate rate on the ^{13}C-NMR time scale at room temperature could account for the apparent broadness of the arene carbon resonances. Studies over a wider temperature range on a higher frequency instrument combined with detailed line-shape analysis will probably be necessary to provide further information. Like $[Cr(CO)_2(PPh_3)(\eta^6\text{-}C_6Et_6)]$,[2,4] complexes **4** and **5** adopt an all-distal arrangement of ethyl groups and the temperature-independence of their NMR spectra indicates cessation of ethyl group rotation consistent with retention of the all-distal arrangement in solution. Presumably, steric repulsion between the phosphine substituents and the proximal ethyl groups is sufficient to overcome the repulsion between mutually distal groups. In contrast to **4**, however, the ethyl groups in $[Cr(CO)_2(PMe_3)(\eta^6\text{-}C_6Et_6)]$ adopt predominantly a 1,3-proximal-2,4,5,6-distal arrangement in the solid state, although there is a small proportion of the 1-proximal-2,3,4,5,6-distal conformer in the lattice.[42] Moreover, in solution these conformers co-exist with the 1,3,5-proximal-2,4,6-distal and all-distal compounds. Since the M–P and M–C (arene) distances in **4** and in $[Cr(CO)_2(L)(\eta^6\text{-}C_6Et_6)]$ (L = PMe_3,[42] PEt_3 [32]) are very similar, there is no obvious reason based on steric effects for these differences.

Experimental

All operations were performed under argon with use of standard Schlenk techniques. Pentane, hexane, thf, diethyl ether, benzene and toluene were pre-dried over sodium wire, distilled from sodium–benzophenone under nitrogen, and stored under nitrogen or argon. Hex-3-yne was degassed before use and stored under argon. Dichloromethane was distilled from CaH_2; acetone and methanol were dried over 3 Å molecular sieves. The complex $[Ru(\eta^6\text{-}C_{10}H_8)(\eta^4\text{-}1,5\text{-COD})]$ was prepared by a literature method.[14]

NMR (^{1}H, ^{13}C and ^{31}P) spectra were measured on Varian XL 200, VXR 300 and Gemini 300 BB spectrometers (Canberra) and on Varian Gemini 200 and VXR 300 spectrometers (Pisa). Chemical shifts are reported relative to internal Me_4Si (^{1}H, ^{13}C) and to external 85% H_3PO_4 (^{31}P). The ^{35}Cl NMR spectra were measured with a Varian VXR 300 instrument at an operating frequency of 29.396 MHz with a spectral window of 100,000 Hz on solutions containing *ca.* 15 mg of compound in 0.5 cm^3 of solvent. Times to collect enough scans for a spectrum ranged from 5 min for $[Et_4N]Cl$ in CD_2Cl_2 to several hours for $[RuCl_2(\eta^6\text{-}C_6Et_6)]_2$ **2** in CD_2Cl_2. Mass spectra were recorded on a VG Micromass 7070 spectrometer (EI, 70 eV) or on a VG ZAB2-SEQ spectrometer (FAB, positive ion). Infrared spectra were measured on Perkin-Elmer 683 or Perkin-Elmer FTIR 1800 spectrometers. Spectra in the range 450–150 cm^{-1} were measured on the latter, either as polythene discs or as CH_2Cl_2 solutions, in a polythene cell of 0.1 mm path length. Elemental analyses were carried out by the staff at the Australian National University Analytical Services Unit, Canberra and of the Facoltà di Farmacia, Università di Pisa. The former also performed a molecular weight determination on complex **2** by means of a Knauer vapour pressure osmometer.

Conductivities were measured on a digital conductivity meter LF DIGI 550 from Wissenschaft-Technische Werkstätten with a CDC 344 platinum electrode from Radiometer. The cell constant was determined by calibration with a standard aqueous solution of KCl. The Λ_0 values were obtained from a plot of Λ_M against the square root of concentration. The linear portion of the graph was extrapolated and Λ_0 was taken as the intercept with the axis where the concentration was zero.

Preparations

$[Ru(\eta^6\text{-}C_6Et_6)(\eta^4\text{-}1,5\text{-COD})]$ 1. A solution of $[Ru(\eta^6\text{-}C_{10}H_8)(\eta^4\text{-}1,5\text{-COD})]$ (0.20 g, 0.59 mmol) in THF (10 cm^3) was treated with hex-3-yne (0.4 cm^3, 3.52 mmol) and the mixture was stirred at room temperature for 3 h. The solvent was evaporated *in vacuo* and the residue was dissolved in *n*-pentane (10 cm^3). The dark brown solution was transferred to an alumina column (20 × 1.5 cm, activity III). The yellow band that eluted with *n*-pentane was concentrated under reduced pressure to a volume of *ca.* 5 cm^3 and set aside at −78 °C to give pale yellow, air sensitive crystals of **1** (0.25 g, 93%). ^{1}H NMR (C_6D_6, 23 °C, 200 MHz) δ 2.76 (br s, 4 H, =CH), 2.36 (br s, 8 H, CH_2 of COD), 2.1 (q, 12H, ^3J = 7.5 Hz, CH_2 of C_6Et_6), 1.82 (t, 18 H, CH_3); (CD_2Cl_2, 23 °C, 200 MHz) δ 2.48 (m, 4 H, =CH), 2.24 (q, 12 H, ^3J = 7.5 Hz, CH_2 of C_6Et_6), 2.04 (m, 4 H, CH*H* of COD), 1.88 (m, 4 H, C*H*H of COD), 1.30 (t, 18 H, ^3J = 7.5 Hz, CH_3); (CD_2Cl_2, −100 °C, 200 MHz) δ 2.32 (br s, 8 H, =CH, proximal CH_2 of C_6Et_6), 2.04, 1.87 (dq, 8 H, distal CH_2 of C_6Et_6), 1.92 (br m, 4 H, CH*H* of COD), 1.72 (approx d, 4 H, C*H*H of COD), 1.36 (br t, 6 H, proximal CH_3), 1.14 (t, 12 H, distal CH_3); ^{13}C-{^{1}H}NMR (C_6D_6, 23 °C, 75.4 MHz) δ 103.4(C_6), 64.3 (=CH), 34.6 (CH_2 of COD), 21.1 (CH_2 of C_6Et_6); (CD_2Cl_2, −100 °C, 75.4 MHz) δ 105.0 (1), 102.0 (2) (C_6), 62.5 (=CH), 34.6 (CH_2 of COD), 21.2–20.8 (overlapping distal CH_2, proximal CH_3 of C_6Et_6), 20.0 (proximal CH_2 of C_6Et_6), 15.8 (distal CH_3 of C_6Et_6); EI-MS (70 eV) *m*/*z* 456 (M^+). Anal. Found: C, 68.7; H, 9.0. $C_{26}H_{42}Ru$ requires: C, 68.6; H, 9.2%.

$[RuCl_2(\eta^6\text{-}C_6Et_6)]_2$ 2. A stirred solution of freshly prepared **1** (0.19 g, 0.40 mmol) in acetone (10 cm^3) was treated dropwise with conc. aq. HCl (0.3 cm^3). The colour changed from yellow to orange-brown. After 30 min the orange air-stable precipitate of **2** was separated by filtration, washed with acetone, and dried *in vacuo*. The yield was 0.16 g (95%). The same complex was obtained similarly in 87% yield from **1** (50 mg, 0.11 mmol) in hexane (*ca.* 100 cm^3) and conc. aq. HCl. Single crystals of **2** suitable for X-ray structural analysis were obtained by layering a CH_2Cl_2/diethyl ether solution with hexane over a 3 d period. The red cubic crystals lost solvent on exposure to air. ^{1}H NMR (CD_2Cl_2, 23 °C, 300 MHz) δ 2.40 (q, 12 H, ^3J = 8 Hz, CH_2), 1.30 (t, 18 H, CH_3); (CD_3CN, 23 °C, 200 MHz) δ 2.50 (q, 12 H, ^3J = 7.6 Hz, CH_2), 1.35 (t, 18 H, CH_3); (CD_2Cl_2, −59 °C, 300 MHz) δ 2.45 (q, 6 H, ^3J = 8 Hz, CH_2), 2.14 (q, 6 H, ^3J = 8 Hz, CH_2), 1.28 (t, 9 H, CH_3), 1.18 (t, 9 H, CH_3); ^{13}C-{^{1}H} NMR (CD_2Cl_2, 23 °C, 75.4 MHz) δ 94–95 (br, C_6), 21.1 (CH_2), 14.7 (CH_3); (CD_2Cl_2, −59 °C, 75.4 MHz) δ 101.7 (1), 87.6 (1) (C_6), 22.7, 20.0, 17.3, 11.3 (CH_2, CH_3); EI-MS (70 eV) *m*/*z* 800 (M^+ − Cl, 420 [$RuCl_2(C_6Et_6)^+$]. Anal. Found: C, 51.45; H, 7.4; Cl, 16.8; *M* (osmometry, CH_2Cl_2, 37 °C, 1.6198 mg cm^{-3}), 670; $C_{36}H_{60}Cl_4Ru_2$ requires: C, 51.7; H, 7.2; Cl 17.0%; *M*, 837.

$[Ru_2Cl_3(\eta^6\text{-}C_6Et_6)_2]PF_6$ [3]PF_6. Solid NH_4PF_6 was added slowly to a stirred solution of complex **2** (50 mg, 0.06 mmol) in ethanol or methanol (3 cm^3) until no more would dissolve. When the solution was set aside without stirring for 3 d, red cubic crystals of **[3]**PF_6 deposited that were of X-ray quality. The supernatant liquid was removed and the crystals were washed by decantation with hexane and cold ethanol. The yield was 44 mg (78%). ^{1}H NMR (CD_3OD, 23 °C, 200 MHz) δ 2.50 (q, 12 H, ^3J = 7.6 Hz, CH_2), 1.33 (t, 18 H, CH_3); ^{13}C-{^{1}H} NMR

Table 6 Crystal and structure refinement data for complexes **1**–**5**

	1	**2**	**3**	**4**	**5**
Compound	$C_{26}H_{42}Ru$	$C_{36}H_{60}Cl_4Ru_2$	$C_{36}H_{60}Cl_3F_6PRu_2$	$C_{21}H_{39}Cl_2PRu.H_2O$	$C_{36}H_{45}Cl_2PRu.C_6H_6$
M	455.67	836.82	946.33	512.50	758.81
Crystal system	Triclinic	Monoclinic	Triclinic	Monoclinic	Orthorhombic
Space group	$P\bar{1}$ (no. 2)	$P2_1/n$ (no. 14)	$P\bar{1}$ (no. 2)	$P2_1/m$ (no. 11)	$P2_12_12_1$ (no. 19)
a/Å	9.578(3)	10.900(3)	13.913(3)	8.698(2)	9.358(2)
b/Å	10.712(3)	9.566(3)	14.132(3)	14.618(4)	19.226(1)
c/Å	13.336(4)	18.439(3)	21.625(3)	9.613(2)	20.478(2)
α/°	68.61(3)		90.97(1)		
β/°	84.16(3)	101.99(2)	90.56(1)	99.01(2)	
γ/°	64.32(3)		100.89(2)		
V/Å^3	1145.6(6)	1880.7(7)	4175(1)	1207.1(4)	3684.2(6)
Z	2	2	4	2	4
D_c/g cm^{-3}	1.321	1.478	1.506	1.410	1.368
μ/mm^{-1})	6.92(Mo-Kα)	92.85(Cu-Kα)	10.05(Mo-Kα)	9.45(Mo-Kα)	53.97(Cu-Kα)
F(000)	484	864	1936	536	1584
Reflections measured	4241	3179	15431	2399	3131
Unique reflections(R_{int})	3981(0.0409)	3004(0.053)	14767(0.019)	2246(0.029)	3111
Used reflections	3979[$I > 2\sigma(I)$]	1953[$I > 3\sigma(I)$]	10182[$I > 3\sigma(I)$]	2008[$I > 3\sigma(I)$]	2857[$I > 3\sigma(I)$]
R, R_w(obs.data)	0.040, 0.099[a]	0.039, 0.040[b]	0.037, 0.030[b]	0.028, 0.024[b]	0.025, 0.027[b]
ρ_{max}, ρ_{min}/e Å^3	0.80, −0.62	0.89, −1.07	1.03, −1.13	0.58, −0.44	0.39, −0.23

[a] $R = \Sigma||F_o| - |F_c||/\Sigma|F_o|$; $R_w = \{\Sigma w(|F_o|^2 - |F_c|^2)^2/\Sigma wF_o^2\}^{1/2}$. [b] $R = \Sigma||F_o| - |F_c||/\Sigma|F_o|$; $R_w = \{\Sigma w(|F_o| - |F_c|)^2/\Sigma wF_o^2\}^{1/2}$.

(CD_2Cl_2, 23 °C, 75.4 MHz) δ 93–95 (br, C_6), 21.5 (CH_2), 15.0 (CH_3); (CD_2Cl_2, −59 °C, 75.4 MHz) δ 101.1 (1), 87.1 (1) (C_6), 22.1, 19.4, 16.7, 12.7 (CH_2, CH_3); ^{31}P-{^{1}H} NMR (CD_3OD, 23 °C, 81.0 MHz) δ −142.7 (sept, $^1J_{PF}$ = 708 Hz, PF_6); EI-MS (70 eV) *m*/*z* 383 [$RuCl(C_6Et_6)^+$]. Anal. Found: C, 44.3; H, 6.5. $C_{36}H_{60}Cl_3F_6PRu_2$ requires: C, 45.7; H, 6.3%.

[$RuCl_2(PMe_3)(\eta^6$-$C_6Et_6)$] 4. A suspension of complex **2** (36 mg, 0.43 mmol) in toluene (10 cm^3) was treated with PMe_3 (0.087 cm^3, 0.86 mmol). The mixture was stirred at 60 °C for 2 h to give a deep red solution. This was filtered to remove a small amount of solid and evaporated to dryness *in vacuo*. The orange-red residue was dissolved in the minimum volume of dichloromethane and the solution was layered with hexane. After 12 h at room temperature a crop of red, air-stable, X-ray quality needles of **4** had deposited. The yield was 32 mg (78%). ^{1}H NMR (CD_2Cl_2, 23 °C, 200 MHz) δ 2.40 (q, 12 H, ^3J = 7.6 Hz, CH_2), 1.26 (d, 9 H, $^2J_{PH}$ = 10.4 Hz, PMe_3), 1.08 (t, 18 H, CH_3 of C_6Et_6); ^{13}C-{^{1}H}NMR (CD_2Cl_2, 23 °C, 75.4 MHz) δ 100.5 (C_6), 22.6 (CH_2), 15.2 (d, $^1J_{PC}$ = 34 Hz, PMe_3), 14.9 (CH_3 of C_6Et_6); ^{31}P-{^{1}H} NMR (CD_2Cl_2, 23 °C, 81.0 MHz) δ 3.1; FAB$^+$-MS *m*/*z* 494 (M^+), 459 (M^+ − Cl). Anal. Found: C, 51.0; H, 7.8. $C_{21}H_{39}Cl_2PRu$ requires: C, 51.0; H, 7.95%.

[$RuCl_2(PPh_3)(\eta^6$-$C_6Et_6)$] 5. A solution of **2** (110 mg, 0.13 mmol) in CH_2Cl_2 (*ca*. 10 cm^3) was heated at reflux for 2 h with an excess of PPh_3 (0.15 g, 1.4 mmol). The solution was filtered, evaporated under reduced pressure to *ca*. 1 cm^3, and layered with hexane. After standing overnight the supernatant liquid was removed by decantation from the dark red, air-stable needles of **5** that had deposited. The excess of triphenylphosphine was removed by washing with three 10 cm^3 portions of hexane. The yield of **5** was 83 mg (60%). ^{1}H NMR (CD_2Cl_2, 23 °C, 300 MHz) δ 8.1–7.3 (m, 15 H, PPh_3), 2.26 (q, 12 H, ^3J = 7.5 Hz, CH_2), 1.19 (t, 18 H, CH_3); ^{13}C-{^{1}H} NMR (CD_2Cl_2, 23 °C, 75.4 MHz) δ 136–128 (m, PPh_3), 101.9 (C_6 of C_6Et_6), 22.2 (CH_2), 15.0 (CH_3); ^{31}P-{^{1}H} NMR (CD_2Cl_2, 23 °C, 121.4 MHz) δ 24.0; FAB$^+$-MS *m*/*z* 680 (M^+ − Cl), 645 (M^+ − PPh_3). Anal. Found: C, 62.0; H, 6.7. $C_{36}H_{45}Cl_2PRu$ requires: C, 63.5; H, 6.7%.

X-Ray crystallography

Selected crystal data and details of data collection and structure refinement are in Table 6. The structures were solved by heavy atom Patterson methods (SHELX 86 for **1**,[50] PATTY for **2**–**5**[51]) and expanded by standard Fourier syntheses (SHELX 93 for **1**,[52] DIRDIF 92 for **2**–**5**[51]). Non-hydrogen atoms were refined anisotropically by full-matrix least-squares. In the case of **4** the PMe_3 group refined with one carbon atom disordered equally over two positions. Hydrogen atoms were included in calculated positions except for those on one of the PMe_3 methyl groups [C(10)] in **4**, which were located on a difference map. Calculations were carried out with the PARST program[53] for **1** and the software package TEXSAN[54] for **2**–**5**. Neutral atom scattering factors,[55] the values of $\Delta f'$ and $\Delta f''$,[56] and the mass attenuation coefficients[56] were taken from standard compilations.

CCDC reference numbers 186313–186317.

See http://www.rsc.org/suppdata/dt/b2/b204875m/ for crystallographic data in CIF or other electronic format.

References

1 H. K. Pal and A. C. Guha, *Z. Kristallogr.*, 1935, **92**, 392.
2 D. J. Iverson, G. Hunter, J. F. Blount, J. R. Damewood, Jr. and K. Mislow, *J. Am. Chem. Soc.*, 1981, **103**, 6073.
3 M. J. McGlinchey, *Adv. Organomet. Chem.*, 1992, **34**, 285.
4 G. Hunter, D. J. Iverson, K. Mislow and G. Blount, *J. Am. Chem. Soc.*, 1980, **102**, 5942.
5 B. Mailvaganam, C. S. Frampton, S. Top, B. G. Sayer and M. J. McGlinchey, *J. Am. Chem. Soc.*, 1991, **113**, 1177.
6 H. Le Bozec, D. Touchard and P. H. Dixneuf, *Adv. Organomet. Chem.*, 1989, **29**, 163.
7 M. A. Bennett, in *Comprehensive Organometallic Chemistry II*, ed. M. I. Bruce, E. W. Abel, F. G. A. Stone and G. Wilkinson, Pergamon, Oxford, 1995, vol. 7, p. 550.
8 M. Crocker, M. Green, A. G. Orpen and D. M. Thomas, *J. Chem. Soc., Chem. Commun.*, 1984, 1141.
9 M. Crocker, S. F. T. Froom, M. Green, K. R. Nagle, A. G. Orpen and D. M. Thomas, *J. Chem. Soc, Dalton Trans.*, 1987, 2803.
10 M. A. Bennett, T.-N. Huang, T. W. Matheson and A. K. Smith, *Inorg. Synth.*, 1982, **21**, 74.
11 J. W. Hull, Jr. and W. L. Gladfelter, *Organometallics*, 1984, **3**, 605.
12 M. A. Bennett, L.-Y. Goh, I. J. McMahon, T. R. B. Mitchell, G. B. Robertson and W. A. Wickramasinghe, *Organometallics*, 1992, **11**, 3069.
13 P. Pertici, A. Verrazzani, G. Vitulli, R. Baldwin and M. A. Bennett, *J. Organomet. Chem.*, 1998, **551**, 37.
14 M. A. Bennett, H. Neumann, M. Thomas, X.-Q. Wang, P. Pertici, P. Salvadori and G. Vitulli, *Organometallics*, 1991, **10**, 3237.
15 P. Pertici, G. Vitulli, R. Lazzaroni, P. Salvadori and P. L. Barili, *J. Chem. Soc., Dalton Trans.*, 1982, 1019.
16 M. A. Bennett, I. J. McMahon, S. Pelling, M. Brookhart and D. M. Lincoln, *Orgnametallics*, 1992, **11**, 127.

17 P. A. Wexler, D. E. Wigley, J. B. Koerner and T. A. Albright, *Organometallics*, 1991, **10**, 2319.
18 J. Müller, K. Qiao, R. Schubert and M. Tschampel, *Z. Naturforsch., Teil B*, 1993, **48**, 1558.
19 W. A. Herrmann, W. R. Thiel and E. Herdtweck, *Polyhedron*, 1988, **7**, 2027.
20 H. Schmid and M. L. Ziegler, *Chem. Ber.*, 1976, **109**, 132.
21 S. F. Watkins and F. R. Fronczek, *Acta Crystallogr., Sect. B*, 1982, **38**, 270.
22 F. B. McCormick and W. B. Gleason, *Acta Crystallogr., Sect. C*, 1988, **44**, 603.
23 B. Therrien, T. Ward, M. Pilkington, C. Hoffmann, F. Gilardoni and J. Weber, *Organometallics*, 1998, **17**, 330.
24 H. K. Gupta, P. E. Lock, D. W. Hughes and M. J. McGlinchey, *Organometallics*, 1997, **16**, 4335.
25 F. B. McCormick and W. B. Gleason, *Acta Crystallogr., Sect. C*, 1993, **49**, 1493.
26 F. Grepioni, D. Braga, P. J. Dyson, B. F. G. Johnson, F. M. Sanderson, M. J. Calhorda and L. F. Veiros, *Organometallics*, 1995, **14**, 121.
27 D. A. Tocher and M. D. Walkinshaw, *Acta Crystallogr., Sect. B*, 1982, **38**, 3083.
28 Yu. T. Struchkov and A. S. Batsanov, *Metalloorg. Khim.*, 1988, **1**, 1143.
29 D. S. Pandey, A. N. Sahay, O. S. Sisodia, N. K. Jha, P. Sharma, H. E. Klaus and A. Cabrera, *J. Organomet. Chem.*, 1999, **592**, 278.
30 M. J. McGlinchey, J. L. Fletcher, B. G. Sayer, P. Bougeard, R. Faggiani, C. J. L. Lock, A. D. Bain, C. Rodger, E. P. Kündig, D. Astruc, J. R. Hamon, P. Le Maux, S. Top and G. Jaouen, *J. Chem. Soc., Chem. Commun.*, 1983, 634.
31 S. Denholm, G. Hunter and T. J. R. Weakly, *J. Chem. Soc., Dalton Trans.*, 1987, 2789.
32 G. Hunter, J. F. Blount, J. R. Damewood, Jr., D. J. Iverson and K. Mislow, *Organometallics*, 1982, **1**, 448.
33 M. J. McGlinchey, P. Bougeard, B. G. Sayer, R. Hofer and C. J. L. Lock, *J. Chem. Soc., Chem. Commun.*, 1984, 789.
34 D. R. Robertson, T. A. Stephenson and T. Arthur, *J. Organomet. Chem.*, 1978, **162**, 121.
35 T. Arthur and T. A. Stephenson, *J. Organomet. Chem.*, 1981, **208**, 369.
36 W. J. Geary, *Coord. Chem. Rev.*, 1971, **7**, 81.
37 R. D. Feltham and R. G. Hayter, *J. Chem. Soc.*, 1964, 4587.
38 P. Uguagliati, G. Deganello, L. Busetto and U. Belluco, *Inorg. Chem.*, 1969, **8**, 1625.
39 J. W. Akitt, in *Multinuclear NMR*, ed. J. Mason, Plenum, New York, 1987, ch. 17, p. 447.
40 B. Lindman and S. Forsén, in *NMR and the Periodic Table*, ed. R. K. Harris and B. E. Mann, Academic, London, 1978, ch. 13, p. 421.
41 M. A. Bennett and A. K. Smith, *J. Chem. Soc., Dalton Trans.*, 1974, 233.
42 J. F. Blount, G. Hunter and K. Mislow, *J. Chem. Soc., Chem. Commun.*, 1984, 170.
43 H. Werner and H. Kletzin, *J. Organomet. Chem.*, 1982, **228**, 289.
44 M. A. Bennett, T.-N. Huang and J. L. Latten, *J. Organomet. Chem.*, 1984, **272**, 189.
45 M. R. J. Elsegood and D. A. Tocher, *Polyhedron*, 1995, **14**, 3147.
46 M. A. Bennett, G. B. Robertson and A. K. Smith, *J. Organomet. Chem.*, 1972, **43**, C41.
47 J.-R. Hamon, J.-Y. Saillard, A. Le Beuze, M. J. McGlinchey and D. Astruc, *J. Am. Chem.Soc.*, 1982, **104**, 7549.
48 R. H. Dubois, M. J. Zaworotko and P. S. White, *J. Organomet. Chem.*, 1989, **362**, 155.
49 G. Hunter and K. Mislow, *J. Chem. Soc., Chem. Commun.*, 1984, 172.
50 G. M. Sheldrick, SHELX 86, Program for Crystal Structure Solution, University of Göttingen, 1986.
51 P. T. Beurskens, G. Admiraal, G. Beurskens, W. P. Bosman, S. Garcia-Granda, R. O. Gould, J. M. M. Smits and C. Smykalla, the PATTY and DIRDIF Program System, Technical Report of the Crystallographic Laboratory, University of Nijmegen, Nijmegen, 1992.
52 G. M. Sheldrick, SHELX 93, Program for Crystal Structure Refinement, University of Göttingen, 1993.
53 M. Nardelli, *Comput. Chem.*, 1983, **7**, 95.
54 TEXSAN, Single Crystal Structure Analysis Software, Molecular Structure Corp., The Woodlands, TX, 1985 and 1992.
55 *International Tables for X-ray Crystallography*, The Kynoch Press, Birmingham, England, vol. IV, Table 2.2A, 1974.
56 *International Tables for Crystallography*, Kluwer Academic, Dordrecht, 1992, vol. C.
57 C. K. Johnson, ORTEP, Report ORNL-5138, Oak Ridge National Laboratory, Oak Ridge, TN, 1976.